Relative efficiencies of different ions for producing freely migrating defects

L. E. Rehn, P. R. Okamoto, and R. S. Averback
Materials Science and Technology Division, Argonne National Laboratory, Argonne, Illinois 60439
(Received 16 April 1984)

In situ experimental measurements of radiation-induced segregation rates in a Ni—12.7 at. % Si alloy during irradiation at temperatures from 350 to 650 °C with several different ions are reported. A simple analytical model is used to extract the relative efficiency of each ion for producing freely migrating defects, i.e., those defects which are free to induce microstructural changes. A strong decrease in efficiency is observed with increasing ion mass. Irradiations producing average recoil energies of 1.8, 2.7, 51, and 74 keV are only 48%, 37%, 8%, and $<2\%$ as efficient, respectively, at introducing defects which are free to migrate long distances as an irradiation with a weighted average recoil energy of 730 eV. The results are compared to measurements of defect production efficiencies obtained by other techniques.

INTRODUCTION

Microstructural modifications during irradiation at elevated temperatures are driven primarily by those defects that are free to migrate long distances before annihilation. Hence the production rate of defects that undergo long-range migration must be determined as a function of irradiating particle species and energy before quantitative correlations can be made between microstructural changes induced in different irradiation environments. Such knowledge is important for predicting materials behavior in fission and fusion reactors, as well as for optimizing near-surface materials properties using ion-beam modification techniques.

Experimental determinations of the fraction of defects which escape their parent cascade and migrate substantial distances have been reported using reactor irradiations.[1–3] However, reactors do not permit the systematic analysis of different primary recoil spectra which is required to obtain a detailed understanding of the defect-production process. Ion irradiation, because of its inherent flexibility with respect to particle mass and energy, does allow the effect of very different primary recoil spectra on the defect-production process to be investigated systematically.[4]

As shown by Okamoto *et al.*,[5] the relative efficiencies of different irradiation particles for producing long-range migrating defects can be determined directly from measurements of radiation-induced segregation. Numerous systematic studies of radiation-induced segregation have been performed on binary nickel alloys containing from 1—13 at. % silicon. Interstitial loops coated with Ni_3Si were first reported in irradiated Ni-Si alloys by Barbu and Ardell.[6] Potter *et al.*[7] showed that Ni_3Si coatings also form on the surfaces of these alloys during irradiation at elevated temperature as a result of defect-flux—driven segregation. Parabolic growth, i.e., thickness increasing linearly with the square root of irradiation time at a constant dose rate, was first predicted for the surface coatings by Okamoto,[8] and has been observed experimentally using infrared emissivity, Auger depth profiling,[9] Rutherford backscattering[9,10] (RBS), and stereo electron microscopy.[11]

Previous work has established details of the coating-growth kinetics,[10] and demonstrated a strong influence of irradiation particle mass on the coating thickness.[12] Here we report additional experimental results obtained on a Ni—12.7 at. % Si alloy, and focus on extracting quantitative information about the efficiencies of different ions for producing freely migrating defects at elevated temperatures.

PROCEDURE

In this section the experimental and theoretical procedures are outlined. Various features of the Ni_3Si surface coatings make it possible to determine migrating defect concentrations during irradiation. First, the parabolic growth-rate constant provides a simple, quantitative definition for the rate of long-range atom transport induced by the irradiation. Second, the coating growth is a one-dimensional problem which, with a few reasonable assumptions, can be solved analytically to obtain a relationship between the coating-growth-rate constant and the steady-state concentration of freely migrating defects. Finally, since *changes* in the coating thickness can be measured very accurately ($\pm<1$ nm), relative defect-production efficiencies can be determined quantitatively.

The experimental procedure is as follows. A time sequence of RBS spectra is acquired during ion irradiation at a particular temperature. Sequential spectra are then subtracted from the initial spectrum to yield a series of difference spectra which contain information about the coating thickness as a function of time at constant dose rate. The RBS difference spectra are converted to plots of coating thickness as a function of the square root of irradiation time. The growth-rate constants for the various irradiation conditions are given by the slopes of the resulting straight-line plots. Simultaneous analysis was employed for all light-ion bombardments, i.e., H, He, and Li. Since ions which are more massive than the substrate do not backscatter, coatings grown during heavy-ion irradia-

tions were analyzed with 2-MeV He ions after cooling to room temperature, where no additional segregation occurs. Experimental details can be found elsewhere.[9,10]

In Ni-Si alloys the available evidence strongly supports the idea that the migration of tightly bound interstitial-silicon complexes toward the surface provides the main driving force for coating growth.[13] For tight binding, recombination of vacancies and silicon-interstitial complexes becomes the dominant mode of defect annihilation and, with the exception of the silicon-depleted region immediately beneath the coating, quasi-steady-state concentrations of vacancies and complexes are established quickly, and maintained during most of the coating growth. The tight-binding assumption leads to an analytical approximation for the parabolic growth-rate constant as a function of the steady-state bulk concentration of silicon-interstitial complexes, c_{is}^0. Assuming that the sink concentration remains constant, or negligibly small during the irradiation, Okamoto *et al.*[5] find, for the coating thickness W,

$$W(t)=A(t-t_0)^{1/2}\ , \tag{1}$$

where the growth-rate constant A has units of length/(time)$^{1/2}$, and is given by

$$A=\left[\frac{2c_s^0}{c_s^p(c_s^p-c_s^0)}\right]^{1/2}(D_{is}c_{is}^0)^{1/2}\ . \tag{2}$$

Here, t_0 is the incubation time until the coating first precipitates, c_s^0 is the bulk silicon concentration (in atom fraction), c_s^p is the concentration of silicon in the surface coating, and D_{is} is the diffusion coefficient for the silicon-interstitial complexes. The rate theory of Wiedersich[14] can be used to calculate c_{is}^0. Experimental studies[13] of interstitial-silicon complexes indicate that the complexes are considerably more mobile than the vacancies ($D_{is}\gg D_v$). For this condition it has been shown[5] that at low temperatures, where recombination between interstitial-silicon complexes and irradiation-induced vacancies dominates defect annihilation,

$$A=\left[\frac{2c_s^0}{c_s^p(c_s^p-c_s^0)}\right]^{1/2}\left[\frac{a_0^2D_vK_0}{a_r}\right]^{1/4}\ . \tag{3}$$

K_0 is the actual rate of production of defects which are free to migrate long distances, a_0 is the lattice constant, and a_r is the number of lattice sites in the recombination volume for vacancies and complexes. At high temperatures, where the thermal-equilibrium concentration of vacancies, $\bar{c}_v$, becomes significant,

$$A=\left[\frac{2c_s^0}{c_s^p(c_s^p-c_s^0)}\right]^{1/2}\left[\frac{a_0^2K_0}{a_r\bar{c}_v}\right]^{1/2}\ . \tag{4}$$

These solutions are sketched in the form of an Arrhenius plot ($\ln AK_0^{-1/2}$ versus T^{-1}) in Fig. 1. Both the low- and high-temperature solutions predict Arrhenius behavior for the quantity $AK_0^{-1/2}$, but with different slopes. At low temperatures, the slope becomes equal to minus one-fourth the migration enthalpy of the slowest moving defect (in this case, the vacancy). For higher temperatures, the sign and magnitude of the slope change to equal one-half the vacancy-formation enthalpy.

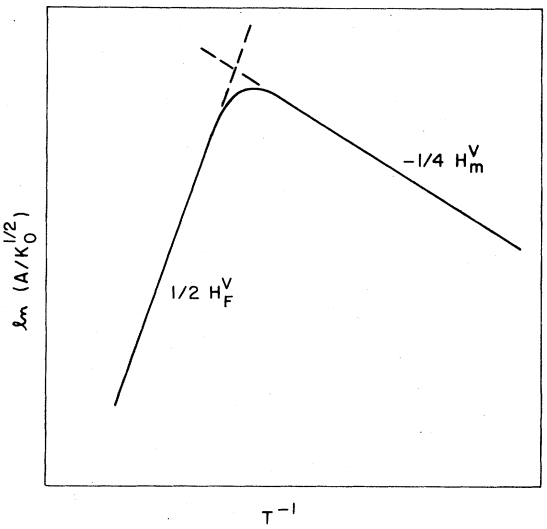

FIG. 1. Schematic Arrhenius plot of the predicted temperature dependence for coating growth.

These solutions also reveal the effect of varying the dose rate (K_0) on the coating-growth-rate constant. The quantity $D_{is}c_{is}^0$ varies as K_0 at high temperature, and $(K_0)^{1/2}$ at low temperatures. The slope of the straight line obtained by plotting coating thickness (W) as a function of the square root of the dose $[(K_0t)^{1/2}]$ should therefore be independent of dose rate at high temperatures, but vary inversely with the fourth root of the dose rate at low temperatures. The validity of these predictions was demonstrated previously.[10,15] Of particular importance to the present objective is the experimental verification of the predicted dose-rate dependence. The correct understanding of the dose-rate dependence of the coating growth means that *relative* defect-production efficiencies can be determined directly from measurements of the growth-rate constants. For this purpose, we define the production efficiency ϵ as

$$\epsilon\equiv K_0/K_{\rm calc}\ , \tag{5}$$

where $K_{\rm calc}$ is the calculated defect-production rate. Since it is only those defects which escape their parent cascade and become free to migrate long distances that contribute to the coating growth, the relative efficiency of two different irradiation particles (1 and 2) for producing long-range migrating defects is, from Eq. (3), in the lower-temperature Arrhenius region,

$$\frac{\epsilon_1}{\epsilon_2}=\frac{K_{\rm calc}^{(2)}}{K_{\rm calc}^{(1)}}\left[\frac{A^{(1)}}{A^{(2)}}\right]^4\ , \tag{6}$$

and, from Eq. (4), in the higher-temperature regime,

$$\frac{\epsilon_1}{\epsilon_2}=\frac{K_{\rm calc}^{(2)}}{K_{\rm calc}^{(1)}}\left[\frac{A^{(1)}}{A^{(2)}}\right]^2\ . \tag{7}$$

RESULTS

Examples of the RBS data collected during irradiation with 1.0-MeV protons at 558 °C are shown in Fig. 2(a).

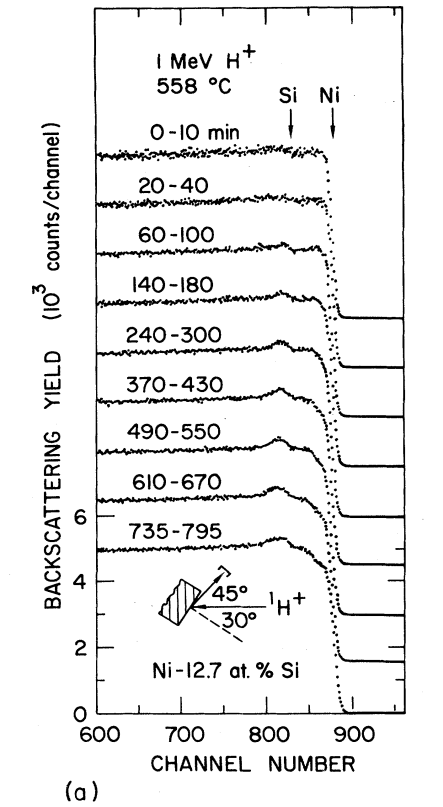

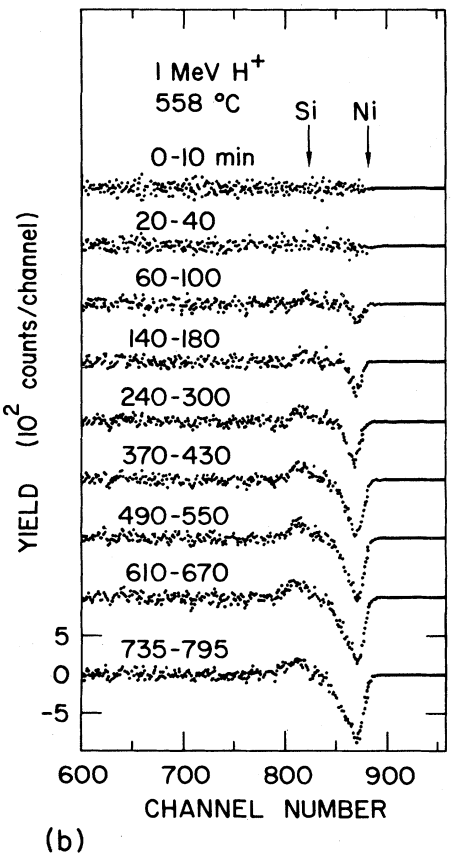

FIG. 2. (a) Series of sequential RBS spectra collected during 1-MeV proton irradiation of a Ni—12.7 at.% Si specimen at 558 °C. (b) Difference spectra obtained from (a).

The differences between the RBS spectra collected over sequential time intervals are displayed in Fig. 2(b). The (0—10)-min difference spectrum in Fig. 2(b) is the difference between the as-collected, initial spectrum and a smoothed spectrum obtained by averaging counts in adjacent channels of the initial spectrum; the smoothing procedure reduces scatter in the difference spectra. Each difference spectrum reveals the change from the smoothed initial spectrum determined during the indicated irradiation interval. All spectra were normalized to correct for variations in acquisition-time and beam-current fluctuations. An RBS computer-simulation program[16] was used to obtain coating thicknesses from the difference spectra. The conversion into thickness, however, is straightforward and can be accomplished without simulation techniques.[17] The layer thicknesses obtained from the difference spectra in Fig. 2(b) are displayed as a function of the square root of the irradiation time in Fig. 3. Data from similar irradiations at 408, 452, 499, and 605 °C are also shown. The slope of the resulting straight line through the data points obtained at a given temperature is the coating-growth-rate constant A for those irradiation conditions. Growth-rate constants have been measured at several temperatures ranging from 350 to 650 °C for the following irradiation particles: 1-MeV ^{1}H, 2-MeV ^{4}He, 2-MeV ^{7}Li, 3-MeV ^{58}Ni, and 3.25-MeV ^{84}Kr. Actual current densities I, calculated cross sections for Frenkel-pair production, σ_{FP}, and corresponding calculated displacement rates in the near-surface region are listed in Table I for all the irradiations. The conversion from ion current density into displacement rate was done via the PINTO computer code.[18] An average displacement threshold energy of 33 eV and a pure-Ni specimen were assumed for the calculations.

The experimental results are displayed in an Arrhenius fashion, $\ln(AK_{calc}^{-1/2})$ as a function of the inverse of the ab-

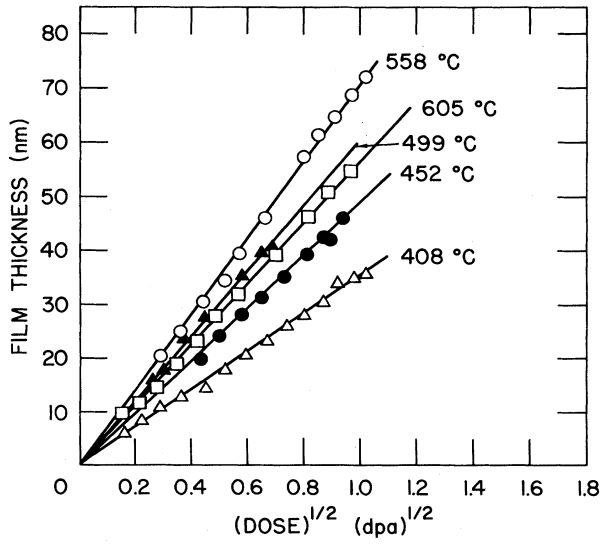

FIG. 3. Measured coating thickness as a function of the square root of the calculated displacements per atom (dpa) during 1-MeV proton irradiation at temperatures of 408, 452, 499, 558, and 605 °C.

TABLE I. Irradiation parameters.

Ion	σ_{FP} (cm^2)	I (μA/cm^2)	K_{calc} (dpa/s)
1.0-MeV ^{1}H	7.0×10^{-20}	65	2.6×10^{-5}
2.0-MeV ^{4}He	6.3×10^{-19}	79	3.1×10^{-4}
2.0-MeV ^{4}He	6.3×10^{-19}	6.6	2.6×10^{-5}
2.0-MeV ^{7}Li	2.4×10^{-18}	24	3.1×10^{-4}
3.0-MeV ^{58}Ni	5.4×10^{-16}	0.20	6.9×10^{-4}
3.25-MeV ^{84}Kr	1.1×10^{-15}	0.045	3.1×10^{-4}

solute irradiation temperature, T^{-1}, in Fig. 4. The division of A by $(K_{calc})^{1/2}$ normalizes all the irradiations to the same calculated rate of defect production and facilitates direct comparison of the results. Only one temperature (520 °C) was investigated using Li ions; a line with the same slope as determined for the other ions has been drawn through this result. The He data exhibit the predicted [cf. Eq. (3)] inverse-fourth-root dependence of the quantity $A/K_0^{1/2}$ on dose rate at lower temperatures, and [cf. Eq. (4)] no dependence on dose rate at higher temperatures. The sharp drop in growth rate (He results, Fig. 4) which occurs for temperatures below ~375 °C is believed to arise from an increased concentration of irradiation-induced internal sinks which compete with the surface for segregating solute.

Figure 4 reveals that for particles of approximately the same energy a large reduction in the measured growth-rate constant occurs with increasing ion mass. This

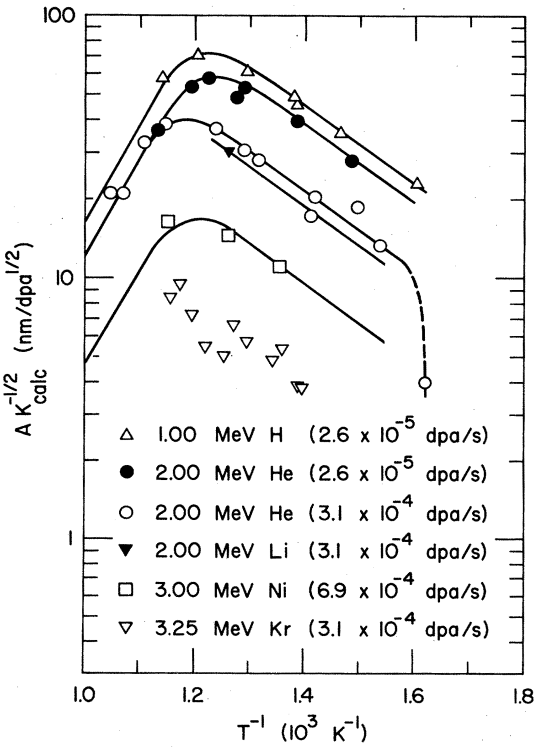

FIG. 4. Arrhenius plot of the measured growth rates A. $K_{calc}^{-1/2}$ of γ coatings on Ni—12.7 at.% Si specimens for different ion irradiations. dpa stands for displacements per atom.

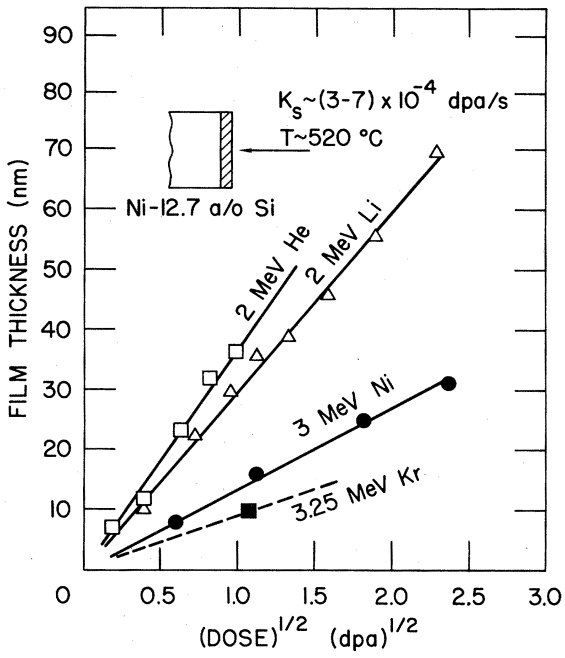

FIG. 5. Coating thicknesses as a function of the square root of the calculated number of displacements per atom (dpa) for irradiations with four different ions at approximately the same energy, calculated dose rate, and temperature.

reduction is demonstrated more directly in Fig. 5, where the coating-growth measurements are plotted for irradiations with four different ions at approximately the same energy (2—3 MeV), dose rate (5×10^{-4} dpa/s, where dpa denotes displacements per atom), and temperature (520 °C). The effects of sputtering and ion-beam mixing of the coating and substrate are both small relative to the growth rate during He irradiation, and thus cannot explain the large decrease observed in the growth-rate constant with increasing ion mass.[5,10]

DISCUSSION

The results (Figs. 4 and 5) presented in the preceding section show clearly that normalizing the different irradiations to approximately the same calculated dpa rate does *not* result in similar growth-rate constants. Hence, microstructural changes induced at elevated temperatures in different irradiation environments cannot be expected to correlate on the basis of normalized dpa rates. The observation that different irradiations cannot be adequately normalized solely on the basis of dpa calculations is not new; it has been noted previously by several authors on the basis of both experimental evidence and theoretical considerations. The underlying reason for the failure of the dpa normalization is quite simple. Displacement calculations determine the total amount of energy which goes into displacing lattice atoms, but they ignore differences in the spatial distribution of the defect production. Since the number of jumps a defect makes before annihi-

lation, i.e., the amount of atom transport or diffusion which occurs, depends strongly on whether the defects are produced in relatively isolated events or in "cascade" regions of locally high defect densities, a more detailed description which takes into account differences in the spatial distribution of defect production during irradiation is required to obtain a correct normalization. Such a description can be inferred from the calculated distribution of energies with which the primary knock-on atoms recoil. This distribution is called the primary-recoil spectrum for an irradiation, and it can be calculated using standard computer codes. Since we are in fact concerned with describing the spatial distribution of the defects which are produced, the function of fundamental interest is the primary-recoil spectrum weighted by the total number of Frenkel-pair defects produced by each primary recoil. To obtain this weighted recoil spectrum, which is discussed in detail in Ref. 4, we need to calculate the fraction of defects produced by all primary-recoil atoms with energies less than P. This fraction, $W(P)$, is given by

$$W(P)=\frac{1}{\nu_t(E)}\int_{P_{\min}}^{P} dP' \frac{d\sigma(E,P')}{dP'}\nu(P') , \tag{8}$$

where

$$\nu_t(E)=\int_{P_{\min}}^{P_{\max}} dP' \frac{d\sigma(E,P')}{dP'}\nu(P') ; \tag{9}$$

$d\sigma(E,P')/dP'$ is the differential cross section for a particle of energy E to produce a primary-recoil atom with energy P', and $\nu(P')$ is the number of Frenkel pairs generated by recoiling lattice atoms of energy P'. The integral in Eq. (8) is evaluated from the average threshold energy for atomic displacements, $P_{\min}$, to energy P. The integral for $\nu_t(E)$, which yields the total cross section for Frenkel-pair production, is evaluated from $P_{\min}$ to $P_{\max}$, the maximum energy transferable from a bombarding ion to a host atom.

$W(P)$ as a function of P is shown in Fig. 6 for the different irradiation particles used in our experiments. Note that the abcissca is plotted as a logarithmic scale. The computer code PINTO was again employed for the calculations; a pure-nickel specimen (average atomic mass of 59 amu) and an average threshold energy of 33 eV were assumed.

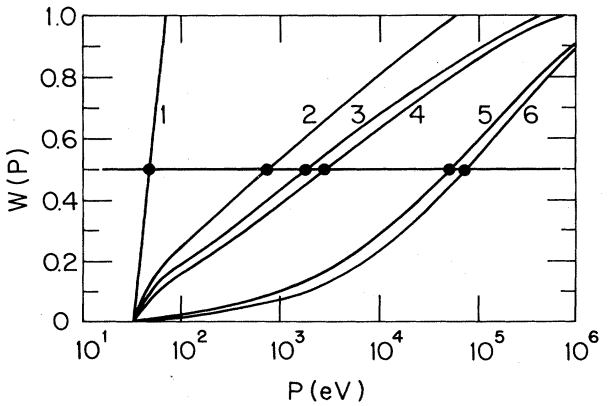

FIG. 6. Calculated fraction of defects produced by primary-recoil events of energy less than P for different irradiation particles: (1) 1-MeV electrons, (2) 1-MeV ^{1}H, (3) 2-MeV ^{4}He, (4) 2-MeV ^{7}Li, (5) 3-MeV ^{58}Ni, and (6) 3.25-MeV ^{84}Kr.

As an example of the information contained in $W(P)$, we first consider the calculated spectrum for 1.0-MeV ^{1}H (Fig. 6). The maximum recoil energy transferred to a lattice atom, $(4m_1m_2)E(m_1+m_2)^{-2}$, is 66 keV, where m_1 and m_2 are the masses of the proton and a nickel atom, respectively. Thus 100% of the defects are produced by primary-recoil events below 66 keV. Fifty percent of the defects are produced by primary-recoil atoms whose energies lie below 720 eV, and 30% by recoils below 150 eV. Of course, no defects are generated by recoils with energies less than the threshold of 33 eV.

Frenkel-pair production was calculated using a modified Kinchin-Pease expression,[19]

$$\begin{aligned} &0, \quad P<P_{\min} \\ &\nu(P)=1, \quad P_{\min}\le P<2.5P_{\min} \\ &\frac{8E_D(P)}{2P_{\min}}, \quad P\ge 2.5P_{\min} \end{aligned} \tag{10}$$

where $E_D(P)$ is the damage energy. As the mass (or to a lesser extent, the energy) of the bombarding ion increases, the primary-recoil spectrum becomes harder. That is, more defects are produced in higher-energy recoil events, increasing the degree of spatial correlation among the defects. However, both experimental and theoretical studies have shown that the spatial correlation among the defects does not increase indefinitely with increasing primary-recoil energy.

Transmission-electron-microscopy studies by Merkle *et al.*[20] first demonstrated that very energetic recoils create closely spaced, but clearly resolvable, subcascade regions. Development of subcascades was postulated by Averback *et al.*[4] to explain their experimental observation of saturation in the low-temperature, irradiation-induced resistivity increment at very high primary-recoil energies. Theoretical calculations of displacement cascades by Jan[21] and by Sigmund,[22] as well as more recent computer-simulation studies by Robinson and Torrens[23] and by Beeler *et al.*[24] also indicate a high probability for subcascade formation at primary-recoil energies above many kilo-electron-volts.

Defect production as a function of primary-recoil energy thus occurs as follows. As recoil events increase in energy from tens to hundred of electrons volts, Frenkel-pair production changes from the introduction of randomly spaced Frenkel defects to the generation of several defect pairs in close proximity. Cascade regions can be clearly distinguished in computer-simulation studies for primary-recoil energies above about 1 keV, and the size of the cascade then continues to increase with increasing energy. For recoils greater than many kilo-electron-volts, the increase in spatial correlation among the defects with increasing recoil energy slows because of the increasing probability for subcascade formation.

No single parameter describes defect production during irradiation as completely as the primary-recoil spectrum does. However, the value of P where $W(P)=0.5$ provides

one measure of the physical "hardness" of a given recoil spectrum. This quantity, i.e., that primary-recoil energy above and below which half of the defects are produced, is referred to as the weighted-average recoil energy ($P_{1/2}$). The weighted-average recoil energy will be used shortly to provide a quantitative summation of the present results. First, however, it is necessary to discuss the experimentally observed decrease in the coating-growth-rate constant with increasing ion mass, i.e., with increasing hardness of the primary-recoil spectrum.

Equations (6) and (7) were used in conjunction with the results presented in Fig. 4 to determine the relative efficiencies of the various ions for producing long-range migrating defects. A computer model of the temperature dependence, which is discussed in more detail by Okamoto *et al.*,[5] was used to obtain "best-fit" lines (cf. Fig. 4) to the data points obtained at different temperatures for each irradiation particle. The model assumes that the defect-production efficiency remains constant over the investigated temperature range (350—650 °C), and a total sink-annihilation probability per defect jump of $\sim 2\times 10^{-4}$. The effect of irradiation-induced sinks on the resultant efficiencies is discussed in Ref. 5, where it is shown that mutual recombination remains the predominant mode of defect annihilation during light-ion irradiation up through the nickel bombardments. Hence, irradiation-induced internal sinks do not significantly affect the efficiency determinations for the proton through nickel data, presumably because most of the defect clusters are thermally unstable at these elevated temperatures. This conclusion is supported by our own electron-microscopy observations of the ion-irradiated specimens, which indicate relatively low sink densities in the region of interest ($\lesssim$200-nm depths). For Kr, however, the experimental evidence[12] indicates that irradiation-induced internal sinks do become significant, particularly for temperatures below $\sim$500 °C. The efficiency reported here for 3.25-MeV Kr was therefore based on the data obtained at temperatures $\gtrsim$550 °C, where the effect of internal sinks is minimal. The relative efficiencies obtained by this procedure are plotted in Fig. 7 as a function of $P_{1/2}$. Note that the efficiency for 1-MeV protons has been set equal to one for convenience. The smooth curve drawn through the data points is meant only as a guide for the eye.

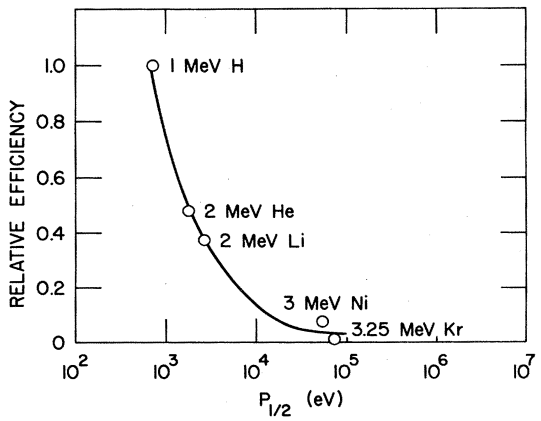

FIG. 7. Relative efficiencies of various ions for producing long-range migrating defects plotted as a function of the weighted-average recoil energy.

Figure 7 provides a quantitative representation of the relative efficiency for producing long-range migrating defects as a function of the "hardness" of the primary-recoil spectrum. Irradiations with weighted-average recoil energies of 1.8, 2.7, 51, and 74 keV are, respectively, only 48%, 37%, 8%, and $<2\%$ as effective as an irradiation with a weighted-average recoil energy of 730 eV for introducing defects which are free to migrate long distances. Note that the abscissa in Fig. 7 is plotted on a logarithmic scale. The most rapid decrease in efficiency occurs over recoil energies up to about 5 keV.

Other experimental techniques have been applied to study defect-production efficiencies in metals as a function of primary-recoil energy. Perhaps the most detailed work was that of Averback *et al.*,[4] who used electrical resistivity measurements to study defect production in copper and silver over a wide range of recoil energies, from about 100 to almost 10^6 eV. They too found a strong decrease in defect-production efficiency with increasing recoil energy up to values of a few kilo-electron-volts. At higher recoil energies the efficiency appeared to saturate. Thus the general shape of their curve was qualitatively the same as the one in Fig. 7. In particular, both studies show that cascade effects become important in the defect-production process at relatively low recoil energies ($\lesssim$1 keV). Before comparing the results in more detail, it is important to recognize that electrical resistivity changes measure the total number of stable defects which are introduced during irradiation. The coating-growth measurements reported here are sensitive only to those defects which are free to migrate long distances, i.e., only some fraction of the total monitored by the resistivity changes.

The resistivity measurements saturated at an efficiency which was still approximately 40% of that found at the lowest primary-recoil energy. In contrast, the apparent limiting value in Fig. 7 is considerably less, only a few percent of the value found at the lowest primary-recoil energy. The observation that the present efficiencies decrease to considerably lower values than the resistivity measurements do implies that the fraction of freely migrating defects is also inversely related to the hardness of the primary-recoil spectrum. Defect interactions within cascades cause the fraction of freely migrating defects to decrease with increasing average recoil energy even faster than the interactions decrease the total number of generated defects.

Another difference between the two studies is the irradiation temperature. In order to retain the maximum number of defects, the resistivity measurements were made at irradiation temperatures below 10 K. The coating-growth measurements were performed at considerably higher irradiation temperatures, between 600 and 1000 K. Differences in defect production can be expected on the basis of this large difference in temperature. For example, a decrease of the displacement threshold energy in copper from 20 eV at room temperature to 12 eV at 575 K has been reported.[25] Consequently, it is quite reasonable that the present relative efficiencies for producing long-range migrating defects at elevated tempera-

tures are qualitatively similar to, but quantitatively different from, the efficiencies for producing stable defects at low temperatures.

The quantitative differences are, however, significant in another context. It has been suggested (see, for example, Ref. 26) that defect-production efficiencies obtained at very low temperatures can be used to correlate microstructural changes induced in different irradiation environments at elevated temperatures. The qualitative agreement between the low-temperature and present results supports this suggestion. However, the fact that quantitative differences exist implies that the relative efficiencies determined from the coating-growth measurements offer a more reliable basis for correlating microstructural changes induced during irradiation at elevated temperatures.

Additional experimental evidence is available in support of the present observation that the relative efficiency for creating long-range migrating defects drops to only a few percent of the initial value as the primary-recoil energy increases from a few hundred electron volts to many kiloelectron-volts. A semiquantitative analysis by Kirk and Blewitt[1] of experimental results by Blewitt *et al.*[27] has shown that fast neutrons (typical recoil energy of ~ 20 keV) are only a few percent as effective as thermal neutrons (typical recoil energy of ~ 300 eV) at producing migrating vacancies in Cu_3Au at 423 K. Goldstone *et al.*[28] have studied dislocation pinning in copper during electron and neutron irradiation at temperatures between 300 and 400 K. They find that fast neutrons in the energy range from 2 to 20 MeV are again only a few percent as effective as (0.5—1)-MeV electrons (average recoil energies < 100 eV) at producing interstitials which migrate to pin dislocations. At considerably lower temperatures (~ 50 K), Schilling *et al.*[3] estimate from resistivity recovery measurements that $\geq 15\%$ of the interstitials produced by fast-neutron irradiation of Cu escape from the displacement cascades. This percentage is in excellent agreement with the results of Theis and Wollenberger,[2] who used resistivity measurements to monitor defect production during reactor irradiations between 50 and 170 K, and report that $\sim 15\%$ of the number of observed interstitials escape any correlated reactions in copper. Since the total number of defects observed by resistivity techniques decreases by about a factor of 3 in going from low-recoil-energy bombardments to reactor irradiations, these latter two studies indicate that the reactor irradiations (typical average recoil energy of 30 keV) are only about 5% as efficient as low-recoil-energy irradiations at creating freely migrating defects.

In a related study, Muroga *et al.*[11] employed stereo-electron-microscopy measurements of coating thicknesses to determine the efficiency of 1-MeV electrons for producing long-range migrating defects in Ni—12.7 at. % Si. Their value shows that the efficiency approximately doubles in going from 1-MeV protons to 1-MeV electrons. From Fig. 6 we see that all defects generated by 1-MeV electrons are created by primary recoils ≤ 80 eV, i.e., the 1-MeV-electron irradiation generates predominantly single, isolated Frenkel pairs. We also note from Fig. 6 that many defects generated by the 1-MeV protons are produced in cascade events. For example, about 25% of the defects are produced in events with energies greater than 5 keV. It is these higher-energy recoil events which presumably are the major factor in reducing the efficiency of 1-MeV protons to only one-half that of 1-MeV electrons.

SUMMARY

Microstructural changes induced during irradiation at elevated temperatures are driven primarily by those defects that escape from their parent cascade and become free to migrate long distances. The present measurements demonstrate that the efficiency for producing long-range migrating defects decreases strongly with increasing primary-recoil energy. Hence microstructural changes in elevated-temperature irradiation environments cannot be correlated solely on the basis of normalized dpa calculations. More importantly, however, the present measurements provide a quantitative basis for normalizing microstructural changes in irradiation environments characterized by widely differing primary-recoil spectra.

ACKNOWLEDGMENTS

We are grateful to H. Wiedersich for his encouragement and for many fruitful discussions throughout the course of this work. The expert technical assistance of P. M. Baldo, B. Kestel, and L. J. Thompson is also gratefully acknowledged. We thank M. A. Kirk for a critical reading of the manuscript. This work was supported by the U.S. Department of Energy.

[1] M. A. Kirk and T. H. Blewitt, Metall. Trans. **9**, 1729 (1978).
[2] U. Theis and H. Wollenberger, J. Nucl. Mater. **88**, 121 (1980).
[3] W. Schilling, G. Burger, K. Isebeck, and H. Wenzl, in *Vacancies and Interstitials in Metals,* edited by A. Seeger, D. Schumacher, W. Schilling, and J. Diehl (North-Holland, Amsterdam, 1970), p. 255.
[4] R. S. Averback, R. Benedek, and K. L. Merkle, Phys. Rev. B **18**, 4156 (1978).
[5] P. R. Okamoto, L. E. Rehn, and R. S. Averback, J. Nucl. Mater. **108-109**, 319 (1982).
[6] A. Barbu and A. J. Ardell, Scr. Metall. **9**, 1233 (1975).
[7] D. I. Potter, L. E. Rehn, P. R. Okamoto, and H. Wiedersich, Scr. Metall. **11**, 1095 (1977).
[8] P. R. Okamoto (unpublished).
[9] L. E. Rehn, R. S. Averback, and P. R. Okamoto, in *Advanced Techniques for Characterizing Microstructures,* edited by F. W. Wiffen and J. A. Spitznagel (The Metallurgical Society of American Institute of Metallurgical Engineers, Warrendale, Pa., 1982), p. 269.
[10] R. S. Averback, L. E. Rehn, W. Wagner, H. Wiedersich, and P. R. Okamoto, Phys. Rev. B **28**, 3100 (1983).
[11] T. Muroga, P. R. Okamoto, and H. Wiedersich, Radiat. Eff. Lett. **68**, 163 (1983).
[12] R. S. Averback, L. E. Rehn, W. Wagner, and P. Ehrhart, J.

Nucl. Mater. **118**, 83 (1983).
[13]L. E. Rehn and P. R. Okamoto, in *Phase Transformations During Irradiation,* edited by F. V. Nolfi, Jr. (Applied Science, Essex, U.K., 1983), Chap. 8.
[14]H. Wiedersich, Radiat. Eff. **12**, 111 (1972).
[15]L. E. Rehn, P. R. Okamoto, R. S. Averback, W. Wagner, and H. Wiedersich, Scr. Metall. **16**, 639 (1982).
[16]R. S. Averback, L. J. Thompson, Jr., J. Moyle, and M. Shalit, J. Appl. Phys. **53**, 1342 (1982); J. F. Ziegler, R. F. Lever, and J. K. Hirvonen, in *Ion Beam Surface Layer Analysis,* edited by O. Meyer, G. Linker, and K. Käppler (Plenum, New York, 1976), p. 163.
[17]See, for example, *Backscattering Spectrometry,* edited by W. K. Chu, J. W. Mayer, and M. A. Nicolet (Academic, New York, 1978).
[18]PINTO was written by Roy Benedek; details can be found in Ref. 4.
[19]G. H. Kinchin and R. S. Pease, Rep. Prog. Phys. **18**, 1 (1955).
[20]K. L. Merkle, Phys. Status Solidi **18**, 73 (1966).
[21]R. J. Jan, Phys. Status Solidi **6**, 925 (1964).
[22]P. Sigmund, Rev. Roum. Phys. **17**, 969 (1972).
[23]M. T. Robinson and I. M. Torrens, Phys. Rev. B **9**, 5008 (1974).
[24]J. R. Beeler, Jr., M. F. Beeler, and C. V. Parks, in *Proceedings of the Conference on Radiation effects and Tritium Technology for Fusion Reactors, Gatlinburg, Tennessee, 1975,* edited by J. S. Watson and F. W. Wiffen (ERDA, Oak Ridge, Tenn., 1976), p. 358.
[25]R. Drosd, T Kosel, and J. Washburn, J. Nucl. Mater. **69-70**, 804 (1978).
[26]P. Jung, B. R. Nielsen, H. H. Anderson, J. F. Bak, H. Knudsen, R. R. Coltman, Jr., C. E. Klabunde, J. M. Williams, M. W. Guinan, and C. E. Violet, in *Effects of Radiation on Materials,* edited by H. R. Brager and J. S. Perrin (American Society for Testing and Materials, Philadelphia, Pa., 1982), p. 963.
[27]T. H. Blewitt, A. C. Klank, T. L. Scott, and W. Weber, in *Radiation-Induced Voids in Metals,* edited by J. W. Corbett and L. C. Ianniello (U.S. Atomic Energy Commission, Oak Ridge, Tenn., 1972).
[28]J. A. Goldstone, D. M. Parkin, and H. M. Simpson, J. Appl. Phys. **51**, 3684 (1980).